A frameshift mutation in the *CHM* gene causes choroideremia with acute angle-closure glaucoma

PINGBO OUYANG[1-3], YUN LI[2,3], FENG ZHANG[2,3], CHENGZHANG ZHU[1], BEIJI ZOU[1], JIANLAN LE[2,3] and LUSI ZHANG[2,3]

[1]School of Information Science and Engineering, Central South University, Changsha, Hunan 410083; [2]Department of Ophthalmology, The Second Xiangya Hospital, Central South University; [3]Department of Ophthalmology, Hunan Clinical Research Center of Ophthalmic Disease, Changsha, Hunan 410011, P.R. China

Received December 4, 2017; Accepted March 22, 2018

DOI: 10.3892/mmr.2018.8851

Abstract. Choroideremia is an X-linked recessive chorioretinal degenerative disease that is characterized by progressive centripetal loss of the photoreceptor, retinal pigment epithelium (RPE), and choriocapillaris layers. The *CHM* gene [choroideremia (Rab escort protein 1)] has been identified as the pathogenic gene in choroideremia. The aim of the present study was to describe the clinical and genetic characteristics of a family with choroideremia family. In the present study, a family with choroideremia presenting with serious chorioretinal atrophy and pigment proliferation, shallow anterior chambers, angle closure and high intraocular pressure (IOP) were recruited. The affected family members underwent a complete ophthalmologic examination. DNA samples obtained from the proband II:1 and the patient II:2 were used for targeted exome sequencing of the *CHM* gene. PCR amplification and Sanger sequencing were used to validate the variations exhibited in family members and controls. A novel frameshift mutation c.280delA (p.Thr94LeufsTer32), in *CHM* was identified in the male proband, the normal carrier I:2 and the phenotyped carrier II:2, which was absent in the normal individual II:3 as well as in 200 normal controls. Comparing the amino acid sequences of *CHM* between multiple species through Clustal Omega indicated conserved amino acids in these mutant sites. Additionally, an X-chromosome inactivation (XCI) assay was performed in the female carriers in the family, in which DNA of the abnormal carrier II:2 and normal carrier I:2 showed a random XCI pattern. To conclude, the present findings strongly indicate that the c.280delA mutation is a disease-causing mutation in our choroideremia pedigree with acute angle-closure glaucoma.

Correspondence to: Dr Lusi Zhang, Department of Ophthalmology, The Second Xiangya Hospital, Central South University, 139 Renmin Middle Road, Changsha, Hunan 410011, P.R. China
E-mail: zhanglusi@csu.edu.cn

Key words: choroideremia, acute angle-closure glaucoma, the *CHM* gene, frameshift mutation, targeted exome sequencing

Introduction

Choroideremia (OMIM: 303100) is an X-linked recessive chorioretinal disorder characterized by progressive degeneration of photoreceptors, retinal pigment epithelium (RPE) and the choroid, with an estimated incidence estimated of 1 in 50,000 to 1 in 100,000 in men (1). Affected hemizygous males usually develop progressive vision loss beginning with night blindness in the first or second decade of their lives, that progresses to reduced function of the peripheral visual fields, and eventually complete blindness later in life (1). Female carriers are often asymptomatic or experience mild symptoms due to X-inactivation (2). However, occasional female carriers can also be fully affected by choroideremia (3).

The molecular basis of choroideremia involves mutation in the *CHM* gene (MIM: 300390) on chromosome Xq21.2. The *CHM* gene contains 15 exons spanning approximately 150 Kb of genomic DNA that encodes a ubiquitously expressed protein, Rab escort protein-1 (REP-1). Until recently, about 300 pathogenic variations of the *CHM* gene have been identified in choroideremia patients (LOVD Retinal and Hearing Impairment Genetic Mutation Database; http://www.lovd.nl/CHM), including small deletions, duplication, nonsense mutations, missense mutations, frameshifts, splice site defects, substitution in the promoter, retrotransposon insertion, and deletion of the entire *CHM* gene (4-6). REP-1 is an essential component of the catalytic Rab geranyl-geranyl transferase (GGTase) II complex, in which it is involved in post-translational isoprenyl modification (7) and intracellular vesicular trafficking (8). REP-1 loss-of-function mutations can be compensated by REP-2 in most tissues; however, REP-2 exhibits less effective geranylgeranylation of Rab27 (9), which plays an important and unique role in regulating vesicular transport in RPE and choriocapillaris cells (10,11). Moreover, REP-1 is particularly crucial for the physical function of RPE and photoreceptors (12,13).

In this study, we conducted a detailed clinical investigation and targeted exome sequencing in a Chinese choroideremia pedigree. A frameshift mutation c.280delA

(p.Thr94LeufsTer32) in *CHM* was detected in the male patients as well as a female carrier. This mutation was absent in the unaffected parents and 200 ethnicity-matched healthy controls. Our findings indicate that this mutation might be an etiological factor of the current pedigree, thus expanding the genetic variation spectrum of choroideremia.

Subjects and methods

Subjects. A choroideremia pedigree from Hunan Province, China, consisting of five members (two males and three females) from two generations (Fig. 1) was recruited by the Second Xiangya Hospital, Central South University (Changsha, China). Ocular examinations, including a slit lamp examination, intraocular pressure (IOP) test, fundus photography (FP), best corrected visual acuity (BCVA) test, A/B-scan ultrasonography, ultrasound biomicroscopy (UBM), optical coherence tomography (OCT), infrared reflectance (IR) imaging, fundus autofluorescence (FAF), and fundus fluorescein angiography (FFA), were performed on these patients. A group of 200 unrelated normal controls who were ethnically matched with the patients were recruited mainly from the hospital and as additional volunteers. This study was approved by the Second Xiangya Hospital Ethics Committee. All of the pedigree members and controls gave their written informed consent complying with the Declaration of Helsinki principles (as revised in Brazil 2013).

Targeted exome sequencing. DNA samples obtained from the proband II:1 and the patient II:2 were used for targeted exome sequencing of the *CHM* gene. Library construction was performed with the custom NimbleGen SeqCap EZ System (Roche NimbleGen, Madison, WI, USA), and 90-cycles paired-end sequencing was performed on Illumina HiSeq2500 Analyzers (Illumina, Inc., San Diego, CA, USA). Illumina Pipeline software (version 1.3.4) was used to perform base-calling and the calculation of quality values for every base.

Reads were aligned to the human reference genome hg19 using Burrows-Wheeler Aligner (BWA, http://bio-bwa.sourceforge.net/). Single nucleotide variation (SNV) and insertion and deletion (indel) identification was performed with SOAPsnp (http://soap.genomics.org.cn/soapsnp.html) and SAMtools (http://samtools.sourceforge.net/). SNVs and indels with read depth ≥8X and Phred score quality ≥30 were reserved and annotated by Annotate Variation (ANNOVAR; http://annovar.openbioinformatics.org/en/latest/user-guide/download/). Multiple sequence alignment was conducted through Clustal Omega (https://www.ebi.ac.uk/Tools/msa/clustalo/) to compare the amino acid sequences of *CHM* between multiple species.

Sanger sequencing. PCR amplification and Sanger sequencing were used to validate the presence of variation. The primer sequences used were as follows: Forward primer, 5'-catgtttca cactgcccact-3', and reverse primer, 5'-aaattcggaggcgttaaggt-3'. PCR was performed in a 10-μl reaction mixture containing 5 μl 2X TaKaRa Taq™ HS Perfect Mix (Takara Biotechnology Co., Ltd., Dalian, China), 30 ng of each primer, and 30 ng of genomic DNA. The amplification conditions consisted of denaturation at 94˚C for 30 sec, followed by 33 cycles of denaturation at 94˚C for 5 sec, annealing at 60˚C for 20 sec and extension at 72˚C for 20 sec. Final extension was performed at 72˚C for 7 min. Sanger sequencing was performed on ABI 3730 DNA Analyzer (Thermo Fisher Scientific, Inc., Waltham, MA, USA).

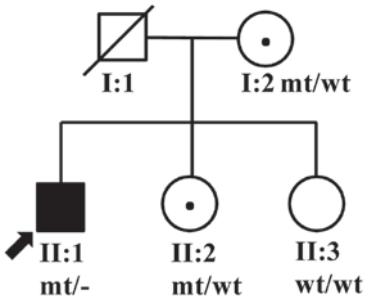

Figure 1. The choroideremia pedigree. Roman numerals refer to generations, and individuals within a generation are numbered from left to right. The proband was noted with an arrow; the filled symbol refers to the patients; the dot symbol refers to carriers; and the open symbol refers to unaffected individuals; wt, wildtype for *CHM* in the individual; mt, *CHM* c.280delA in the individual.

X-chromosome inactivation (XCI) assay. Human androgen receptor gene (NM_000044) and *ZNF261* gene (DXS6673E) were chosen to perform XCI analysis on methylated *HpaII* and/or *Hha*I sites as described previously (14-15). The primers sequences are as follows: NM_000044 forward primer, 5'-GCT GTGAAGGTTGCTGTTCCTCAT-3', and reverse primer, 5'-TCCAGAATCTGTTCCAGAGCGTGC-3'; DXS6673E forward primer, 5'-ATGCTAAGGACCATCCAGGA-3', and reverse primer, 5'-GGAGTTTTCCTCCCTCACCA-3'. The two forward primers were labeled with hexachlorofluorescein fluorescent dye. DNA (2 μg) was digested with 20 units of *Hpa*II or *Hha*I, respectively. Reactions were performed in a 25-μl total volume including 2.5 μl 10X buffer. All incubations were performed for 12 h at 37˚C and then for 20 min at 65˚C. For the PCR reaction, 100 ng DNA was added to a 20-μl PCR reaction mixture containing 0.1 μl ABI Gold Taqase (Applied Biosystems; Thermo Fisher Scientific, Inc.), 2 μl 10X PCR Buffer, 2 μl 25 mM $MgCl_2$, 0.4 μl 10 mM dNTP, 1 μl forward primer, and 1 μl reverse primer. Samples were amplified using a Bio-Rad T100 thermocycler (Bio-Rad Laboratories, Inc., Hercules, CA, USA) for 32 cycles (45 sec at 95˚C, 30 sec at 60˚C, and 30 sec at 72˚C), with initial denaturation at 95˚C for 5 min. The PCR products were separated by capillary electrophoresis on an ABI 3100 DNA analyzer (Applied Biosystems; Thermo Fisher Scientific, Inc.), and were analyzed with GeneMarker® HID software (SoftGenetics, LLC., State College, PA, USA; https://www.softgenetics.com/GeneMarkerHID.php).

Results

Clinical findings. In this family, the proband II:1 was a 46-year-old man who reported having sudden ocular pain and decreased vision in his left eye for one day before he came to our hospital. He also complained of headache and nausea. The BCVA was hand motion in both eyes. The Goldmann IOP of the right eye was 16 mmHg and of the left eye was

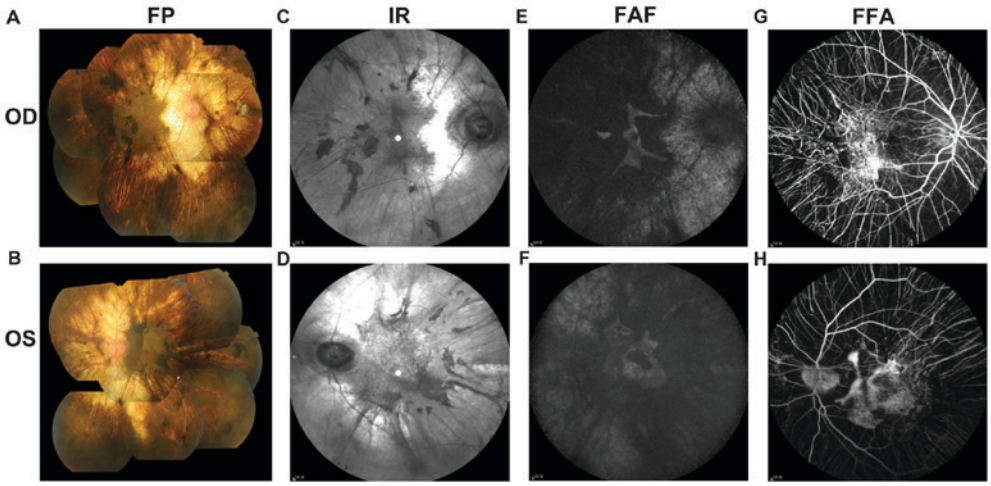

Figure 2. Fundus photography (FP) and infrared reflectance (IR) images of the proband. (A and B) The FP showed that the cup-to-disc ratio was 0.4 oculus dexter (OD) and 0.8 oculus sinister (OS), and identified pink optic nerves and vessel narrowing in both eyes. The color and lustre of the macular was dim, and there was severe chorioretinal atrophy and pigment proliferation in the posterior polar and peripheral fundus in both eyes. (C and D) The IR images demonstrated hyperreflective lesions in the serious chorioretinal atrophy area and hyporeflective lesions corresponding to pigment proliferation. (E and F) Fundus autofluorescence (FAF) showed an isolated area of hyperautofluorescence in the foveal area. Part of the transparent sclera was also observed as hyperreflective tissue. (G and H) Fundus fluorescein angiography (FFA) showed an absence of the choriocapillaris in the region with pigment accumulation and normal retinal vessels.

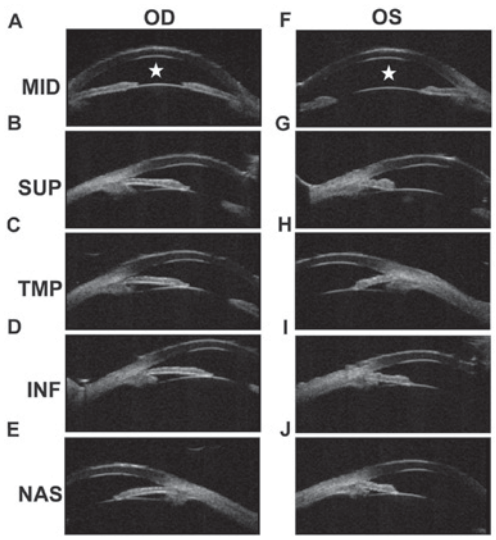

Figure 3. Ultrasound biomicroscopy (UBM) of (A-E) the right eye and (F-J) the left eye of the proband. The shallow depths of the anterior chambers in both eyes were indicated by the white stars. The anterior chamber angles of (B-E) the right eye and part of (J) the left eye were narrow and of (G-I) the left eye were closed. MID, median; SUP, superior side; TMP; temporal side; INF; inferior side; NAS, nasal side.

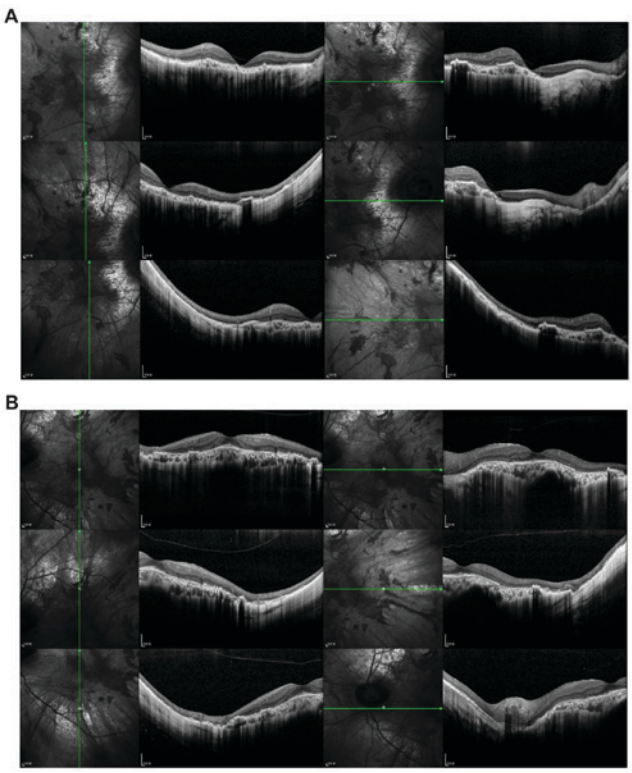

Figure 4. Fundus autofluorescence image demonstrating areas of residual retinal pigment epithelium (RPE) and the corresponding optical coherence tomography image of the proband II:1: (A) left eye and (B) right eye. RPE disruption and pigment hyperplasia were observed except in the central macula in both eyes. An outer retinal tubulation was seen in the fundus. The outer nuclear layer, external limiting membrane and photoreceptor layer were still present in the left fovea.

42 mmHg. The slit-lamp examination identified a shallow anterior chamber and peripheral chambers of <1/4 cornea thickness (CT) in both eyes, and conjunctival congestion and corneal edema in the left eye. The fundus examination results were indicated in Fig. 2. Fundus examination (Fig. 2A and B) identified a cup-to-disc ratio of 0.4 in the right eye and 0.8 in the left eye, pink optic nerves in both eyes, vessel narrowing in both eyes, dimming of the color and lustre of the macular in both eyes, severe chorioretinal atrophy with exposure of the sclera in both eyes, and pigment proliferation in the posterior polar and peripheral fundus in both eyes. The A-scan showed that the axial lengths of the right and left eye were 23.11 and 23.10 mm, respectively. The B-scan showed vitreous opacity in both eyes. UBM of the right eye showed that the anterior chamber depth (ACD) was shallow (Fig. 3A), and also that the anterior chamber angles were narrow at the superior

Table I. Summary of the targeted exome sequencing results.

Sample	Targeted gene	Targeted region (bp)	Targeted region mapped (%)	Targeted exon coverage (%)	Mean depth (x)	Mean depth >30x (%)
II-1	*CHM*	1962	96.00	99.75	210.32	98.45
II-2			95.82	99.26	208.61	95.87

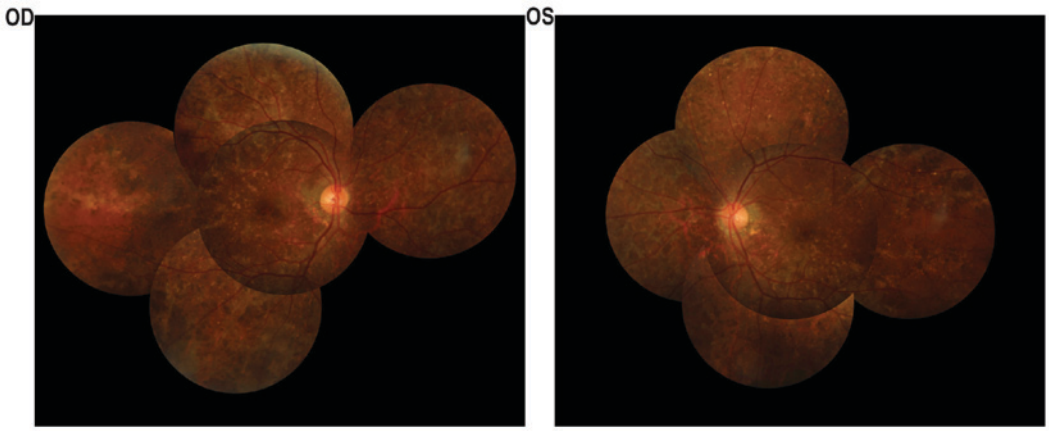

Figure 5. Fundus photographs of the carrier II:2. The fundus photographs revealed that the color and lustre of the retina was darkened, and the retina had a crystal-like appearance. OD, oculus dexter; OS, oculus sinister.

side, the temporal side, the inferior side and the nasal side (Fig. 3B-E). The ACD of the left eye was shallow (Fig. 3F), and was closed at the superior side, the temporal side, and the inferior side (Fig. 3G-I). The angles of the left eye were narrow at the nasal side (Fig. 3J). OCT imaging (Fig. 4) of both eyes indicated widespread disappearance of the choroid and the outer retinal layer, which was accompanied with pigment hyperplasia, though a small part of the choroid was retained in the central macula. In the left fovea, the outer nuclear layer, external limiting membrane, and photoreceptor layer were still present. IR imaging (Fig. 2C and D) demonstrated hyperreflective lesions corresponding to the area of serious chorioretinal atrophy and hyporeflective lesions corresponding to the area of pigment proliferation. FAF (Fig. 2E and F) of both eyes showed an isolated area of hyperautofluorescence in the foveal area. Part of the transparent sclera was also observed as hyperreflective in FAF image. FFA (Fig. 2G and H) of both eyes showed an absence of the choriocapillaris in the regions of pigment accumulation. The retinal vessels were normal in FFA. According to the above information, the patient's clinical diagnosis was choroideremia in both eyes and angle-closure glaucoma (preclinical stage in the right eye, acute attack stage in the left eye).

The proband's sister, II:2, did not report any vision problems, and the anterior segments of both of her eyes were normal. However, the fundus examination identified darkened color and lustre of the retina, and a crystal-like appearance in the retina of both eyes (Fig. 5). The proband's parents, I:1 and I:2, showed no clinical manifestation.

Targeted exome sequencing and sanger validation. We selected the proband II:1 and the patient II:2 for targeted exome sequencing, which was designed to isolate a 1,962-bp DNA region of the *CHM* gene. In our sequencing results, 96.00 and 95.82% of the qualified bases for II:1 and II:2 were mapped to the targeted sequence, with mean read depths of approximately 210.32- and 208.61-fold for II:1 and II:2 (Table I). The exon coverage rates were 99.75 and 99.26% for the patient and female carrier samples, respectively, which was sufficient to pass our thresholds for calling SNVs and indels (Table I). After alignment and variation calling, a total of 12 variations in the *CHM* gene were identified among the two family members, including 2 exonic variations, 9 intronic variations, and 1 in the 3'-UTR (Table II). However, only 1 frameshift variation, c.280delA (p.Thr94LeufsTer32), in *CHM* was found in II:1 and II:2, that had not been reported either in the dbSNP database or in the 1,000 Genomes database, which was predicted to produce a truncated REP-1 protein. Comparing the amino acid sequences of *CHM* between multiple species demonstrated asterisks and codons among the amino acids 94 to 126 (Fig. 6A), which indicated conserved amino acids on these sites.

We used Sanger sequencing to validate the c.280delA variation and analyze the co-segregating status of the variant in all family members. Hemizygous c.280delA variation was found in II:1, and heterozygous c.280delA variations were found in I:2 and II:2, respectively, while the variation was not detected in II:3 (Fig. 6B). The variation was completely cosegregated with the phenotype in all family members except for carrier II:2. In addition, the variation was not identified in the 200 unrelated normal controls. Thus, our results indicate that the variation c.280delA (p.Thr94LeufsTer32) in the *CHM* gene is a genetic etiological factor of the current choroideremia

Table II. Variations detected in *CHM* gene (NM_000325) in the pedigree by targeted exome sequencing.

Position	SNP no.	Variation type	Location	Nucleotide change	Amino acid change	Allele frequency in 1,000 genome	Affected member
chrX:85281760	rs1015148	Hemi, Het	Intron 2	c.116+80C>T	None	0.2024	II-1, II-2
chrX:85281760	rs5923428	Homo	Intron 2	c.116+735A>G	None	0.065	II-2
chrX:85261183	rs62607865	Homo	Intron 2	c.116+21312C>A	None	0.0137	II-2
chrX:85236825		Het	Intron 2	c.117-12delT	None	0	II-2
chrX:85219021	rs10217950	Het	Exon 5	c.351A>G	p.A117A	0.1401	II-2
chrX:85233805		Hemi, Het	Exon 4	c.280 delA	p.T94LfsTer32	0	II-1, II-2
chrX:85215758	rs7880234	Homo	Intron 5	c.703-1776G>A	None	0.0183	II-2
chrX:85212717		Het	Intron 7	c.940+143C>A	None	0	II-1
chrX:85166221~85166222		Het	Intron 9	c.1244+44_+45insATAT	None	0	II-2
chrX:85155596		Hemi	Intron 11	c.1413+55G>T	None	0	II-1
chrX:85145586		Homo	Intron 12	c.1510+3607 A>G	None	0	II-2
chrX:85119508		Hemi	3-UTR	c.*127T>C	None	0	II-1

Homo, homozygous; Het, heterozygous; Hemi, hemizygous.

pedigree. Our phenotype and variation data in this study have been submitted to ClinVar (accession no. SCV000600017).

XCI. Given that the carrier II:2 exhibited disease-related phenotypes, we determined the XCI profile of the female family members. The DNA of the carrier II:2 and normal female I:2 showed 48 and 43% inactivated X chromosome, respectively, indicating that both the female carrier and normal female had a random XCI pattern. Thus, no correlation between phenotypic status and X-inactivation pattern was established in these females.

Discussion

Choroideremia is an X-linked, recessive, chorioretinal degenerative disease characterized by progressive centripetal loss of the photoreceptor, retinal RPE and choroid layers. Our initial patient (II:1) revealed exhibited choroideremia with acute angle-closure glaucoma. Subsequently, in our female carrier II:2, we identified darkening of the color and lustre of the retina, along with a crystal-like appearance of the retina was observed, which was likely due to hypopigmentation of the RPE. These clinical manifestations were similar to phenotypes reported in other studies (16,17) with the exception of the presentation of acute angle-closure glaucoma. II:2 also exhibited narrow or closed anterior chamber angles in both eyes, which may lead to high IOP and acute angle-closure glaucoma in the future.

A novel frameshift variant, c.280delA (p.Thr94LeufsTer32), was identified in the *CHM* gene through targeted exome sequencing in our pedigree, and was validated by Sanger sequencing. The variant was detected in the mother I:2, and in the offspring II:1 and II:2, and thus the proband and the female carrier inherited the variant from their carrier mother rather than acquiring it from a *de novo* germline mutation. As with phenotyped carriers reported in other studies (17,18), our variant was completely cosegregated with the phenotypes. Moreover, our data revealed that both a normal female and a carrier had random XCI patterns, which suggested that there is no preferential XCI of the mutant X chromosome allele. This result is consistent with a previous study of XCI detection in 13 heterozygous females from two families (19).

Other previous studies have suggested that the molecular basis of choroideremia may involve selective underprenylation of Rab protein due to the absence of REP-1 (20). Our frameshift mutation was predicted to create a premature stop codon and to thus lead to a lack of full-length REP-1. In turn, this would likely lead to a deficiency of GGTase function, with the insufficient transfer of geranylgeranylpyrophosphate groups onto Rab proteins potentially resulting in abnormal protein function, preventing their participation in intracellular vesicular transport (21). This would ultimately cause several ocular defects as observed in our patients.

In conclusion, our results suggest that c.280delA (p.Thr94LeufsTer32) in *CHM* was a pathogenic mutation in the present choroideremia family as determined by captured exome sequencing. Such targeted exome sequencing technology may provide a promising tool for genetics testing and counseling among families with choroideremia. Further

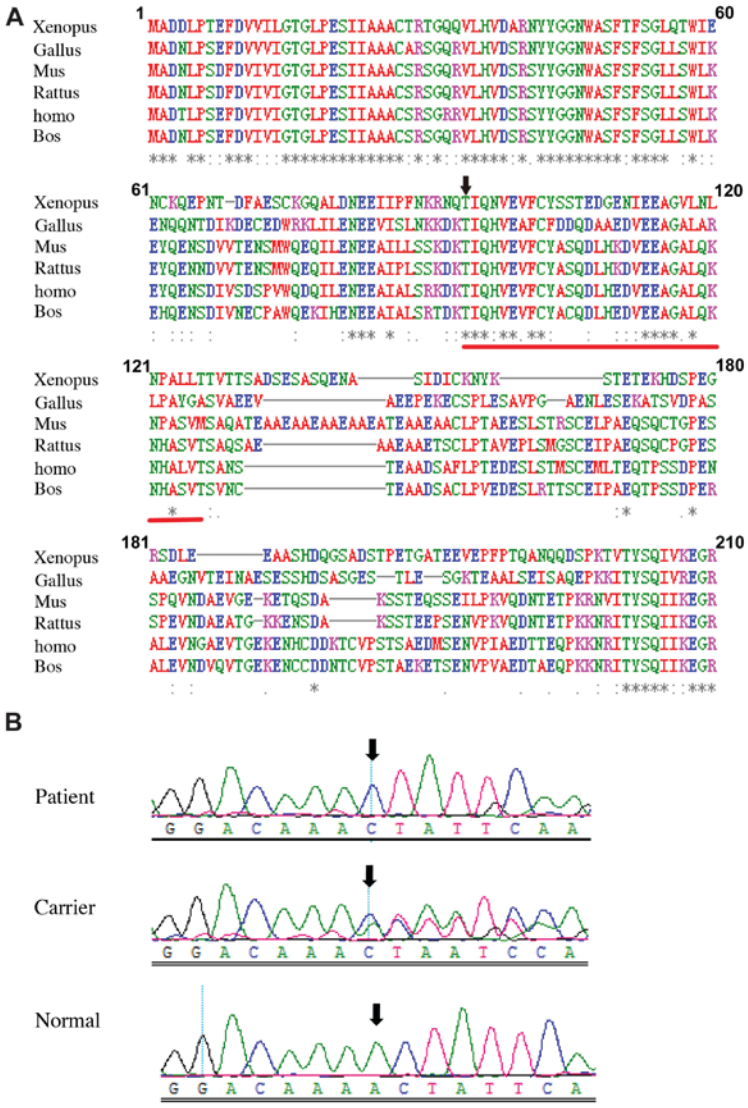

Figure 6. DNA sequence analysis of the *CHM* c.280delA (p.T94LfsTer32) mutation. (A) Evolutionary conservation analysis of p.T94LfsTer32 residues. Asterisk, completely conserved amino acid; codon, highly conserved amino acid; dot, moderately conserved amino acid; red line, mutated amino acid residues. (B) The DNA sequence of the *CHM* c.280delA mutation in the choroideremia pedigree. The arrow indicates the mutated base.

functional and animal studies on the mutant protein will be required to interpret its role in the pathogenesis of the disease.

Acknowledgements

Not applicable.

Funding

This study was supported by the Natural Science Foundation of Hunan Province Project (grant no. 14JJ3041), the National Natural Science Foundation of China (grant nos. 81700837, 81300798, and 61573380), and Department of Science and Technology, Hunan (grant no. 2015TP2007).

Availability of data and materials

Our phenotype and variation data in this study are available from ClinVar (https://www.ncbi.nlm.nih.gov/clinvar/; accession no. SCV000600017). Other datasets used and/or analyzed during the current study are available from the corresponding author on reasonable request.

Authors' contributions

PO, FZ, CZ, and BZ performed the genetic studies, participated in the sequence alignment and analyzed the data. YL and JL participated in the sample collection and clinical examination. LZ designed and supervised the study. LZ and PO wrote the manuscript. All authors read and approved the final manuscript.

Ethical approval and Informed consent

All procedures performed in studies involving human participants were in accordance with the ethical standards of the Second Xiangya Hospital Ethics Committee and with the 1964 Helsinki declaration and its later amendments or comparable ethical standards. Informed consent was obtained from all individuals participants included in the study.

Consent for publication

The patient, the family members and the normal control subjects provided their written informed consents for the publication of any associated data and accompanying images.

Competing interests

All authors declare that they have no competing interests.

References

1. Coussa RG and Traboulsi EI: Choroideremia: A review of general findings and pathogenesis. Ophthalmic Genet 33: 57-65, 2012.
2. Rudolph G, Preising M, Kalpadakis P, Haritoglou C, Lang GE and Lorenz B: Phenotypic variability in three carriers from a family with choroideremia and a frameshift mutation 1388delCCinsG in the REP-1 gene. Ophthalmic Genet 24: 203-214, 2003.
3. Renner AB, Kellner U, Cropp E, Preising MN, MacDonald IM, van den Hurk JA, Cremers FP and Foerster MH: Choroideremia: Variability of clinical and electrophysiological characteristics and first report of a negative electroretinogram. Ophthalmology 113: e1-e10, 2006.
4. van den Hurk JA, van de Pol DJ, Wissinger B, van Driel MA, Hoefsloot LH, de Wijs IJ, van den Born LI, Heckenlively JR, Brunner HG, Zrenner E, *et al*: Novel types of mutation in the choroideremia (CHM) gene: A full-length L1 insertion and an intronic mutation activating a cryptic exon. Hum Genet 113: 268-275, 2003.
5. Radziwon A, Arno G, K Wheaton D, McDonagh EM, Baple EL, Webb-Jones K, G Birch D, Webster AR and MacDonald IM: Single-base substitutions in the CHM promoter as a cause of choroideremia. Hum Mutat 38: 704-715, 2017.
6. Edwards TL, Williams J, Patrício MI, Simunovic MP, Shanks M, Clouston P and MacLaren RE: Novel non-contiguous exon duplication in choroideremia. Clin Genet 93: 144-148, 2018.
7. Leung KF, Baron R and Seabra MC: Thematic review series: Lipid posttranslational modifications. geranylgeranylation of Rab GTPases. J Lipid Res 47: 467-475, 2006.
8. Ali BR and Seabra MC: Targeting of Rab GTPases to cellular membranes. Biochem Soc Trans 33: 652-656, 2005.
9. Larijani B, Hume AN, Tarafder AK and Seabra MC: Multiple factors contribute to inefficient prenylation of Rab27a in Rab prenylation diseases. J Biol Chem 278: 46798-46804, 2003.
10. Futter CE, Ramalho JS, Jaissle GB, Seeliger MW and Seabra MC: The role of Rab27a in the regulation of melanosome distribution within retinal pigment epithelial cells. Mol Biol Cell 15: 2264-2275, 2004.
11. Seabra MC, Ho YK and Anant JS: Deficient geranylgeranylation of Ram/Rab27 in choroideremia. J Biol Chem 270: 24420-24427, 1995.
12. Tolmachova T, Anders R, Abrink M, Bugeon L, Dallman MJ, Futter CE, Ramalho JS, Tonagel F, Tanimoto N, Seeliger MW, *et al*: Independent degeneration of photoreceptors and retinal pigment epithelium in conditional knockout mouse models of choroideremia. J Clin Invest 116: 386-394, 2006.
13. Tolmachova T, Wavre-Shapton ST, Barnard AR, MacLaren RE, Futter CE and Seabra MC: Retinal pigment epithelium defects accelerate photoreceptor degeneration in cell type-specific knockout mouse models of choroideremia. Invest Ophthalmol Vis Sci 51: 4913-4920, 2010.
14. Allen RC, Zoghbi HY, Moseley AB, Rosenblatt HM and Belmont JW: Methylation of HpaII and HhaI sites near the polymorphic CAG repeat in the human androgen-receptor gene correlates with X chromosome inactivation. Am J Hum Genet 51: 1229-1239, 1992.
15. Beever C, Lai BP, Baldry SE, Peñaherrera MS, Jiang R, Robinson WP and Brown CJ: Methylation of ZNF261 as an assay for determining X chromosome inactivation patterns. Am J Med Genet A 120A: 439-441, 2003.
16. Li S, Guan L, Fang S, Jiang H, Xiao X, Yang J, Wang P, Yin Y, Guo X, Wang J, *et al*: Exome sequencing reveals CHM mutations in six families with atypical choroideremia initially diagnosed as retinitis pigmentosa. Int J Mol Med 34: 573-577, 2014.
17. Renner AB, Fiebig BS, Cropp E, Weber BH and Kellner U: Progression of retinal pigment epithelial alterations during long-term follow-up in female carriers of choroideremia and report of a novel CHM mutation. Arch Ophthalmol 127: 907-912, 2009.
18. Zhou Q, Liu L, Xu F, Li H, Sergeev Y, Dong F, Jiang R, MacDonald I and Sui R: Genetic and phenotypic characteristics of three Mainland Chinese families with choroideremia. Mol Vis 18: 309-316, 2012.
19. Perez-Cano HJ, Garnica-Hayashi RE and Zenteno JC: CHM gene molecular analysis and X-chromosome inactivation pattern determination in two families with choroideremia. Am J Med Genet A 149A: 2134-2140, 2009.
20. Esposito G, De Falco F, Tinto N, Testa F, Vitagliano L, Tandurella IC, Iannone L, Rossi S, Rinaldi E, Simonelli F, *et al*: Comprehensive mutation analysis (20 families) of the choroideremia gene reveals a missense variant that prevents the binding of REP1 with Rab geranylgeranyl transferase. Hum Mutat 32: 1460-1469, 2011.
21. Baron RA and Seabra MC: Rab geranylgeranylation occurs preferentially via the pre-formed REP-RGGT complex and is regulated by geranylgeranyl pyrophosphate. Biochem J 415: 67-75, 2008.